# Supplementary Information

# Atomic View of Filament Growth in Electrochemical Memristive Elements

**Hangbing Lv[1, 2], Xiaoxin Xu[1, 2], Pengxiao Sun[1, 2], Hongtao Liu[1, 2], Qing Luo[1, 2], Qi Liu[1, 2], Writam Banerjee[2], Haitao Sun[1, 2], Shibing Long[1, 2], Ling Li[1, 2] & Ming Liu*[1, 2]**

[1]Key Laboratory of Microelectronics Devices and Integrated Technology, Institute of Microelectronics, Chinese Academy of Sciences, Beijing, 100029, China;

[2]Lab of Nanofabrication and Novel Devices Integration Technology, Institute of Microelectronics, Chinese Academy of Sciences, Beijing, 100029, China

Correspondence and requests for materials should be addressed to M.L. (email: liuming@ime.ac.cn)

**Table of Contents:**

**S1. Device structure and equivalent circuit of 1T1R cell.**

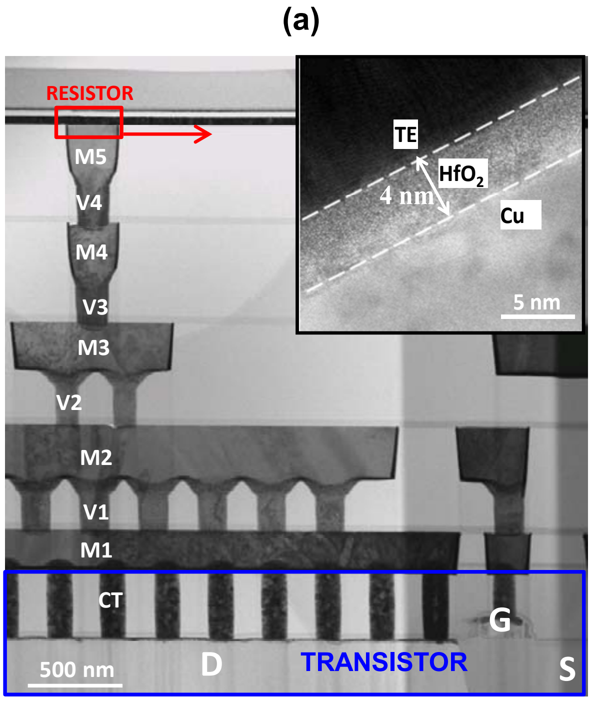


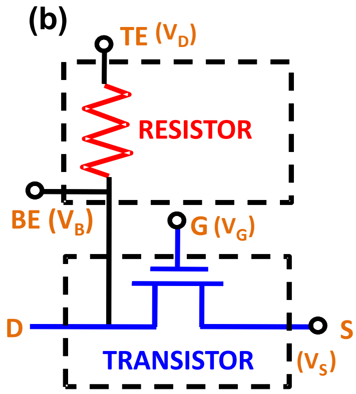


(c)

| | HRS to LRS | LRS to HRS |
|---|---|---|
| $V_D$ | GND | + |
| $V_G$ | + | + |
| $V_S$ | + | GND |

**Figure S1.** (a) The cross-section TEM image of 1T1R structure. The memristive element with Cu/HfO2/Pt structure is fabricated on the top of the transistor. The Cu plug, which connects the drain of transistor, serves as bottom electrode after CMP. The insert is magnification of Cu/$HfO_2$/Pt structure. The $HfO_2$ layer is about 4 nm. (b) Equivalent circuit of 1T1R cell. (c) Operation conditions. Positive voltage bias on Cu electrode is needed to perform the forming and SET operation with the Pt electrode grounded. For RESET operation, the voltage polarity should be opposite. In the case of 1T1R structure here, the $V_S$ and $V_D$ should be positively biased for forming/SET and RESET, respectively.

**S2. Multi-level storage achieved by the varied gate voltage.**

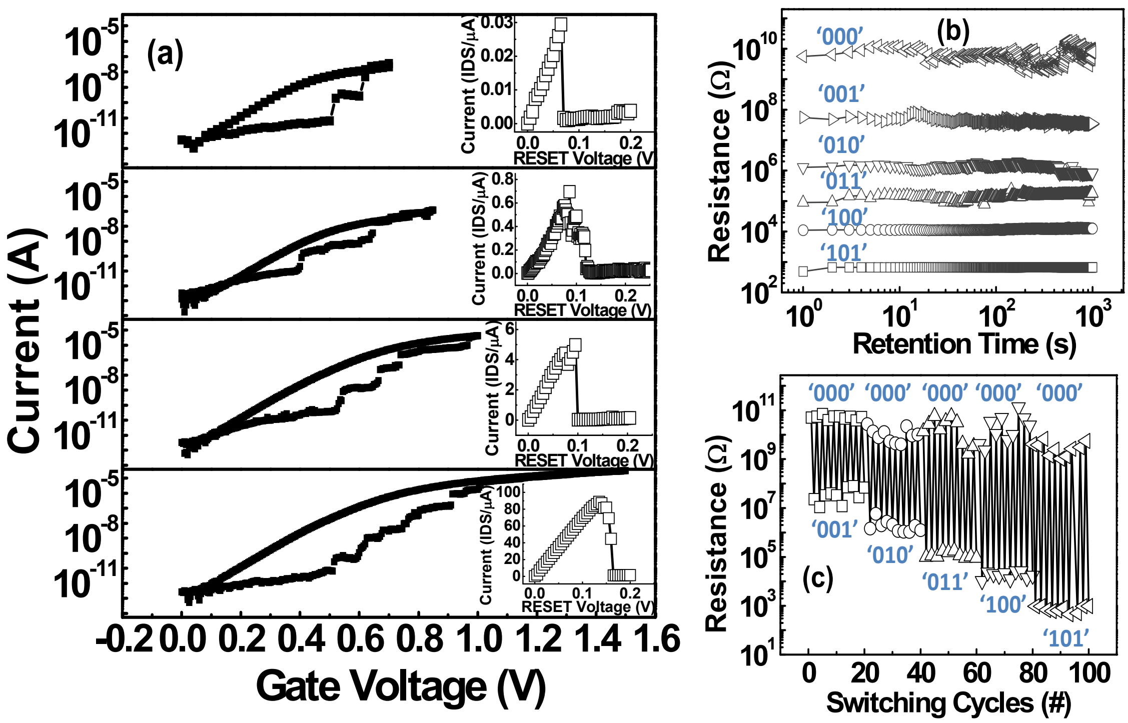


**Figure S2.** (a) The curves of $I_{ds}$ verse $V_G$. The cell resistance can be precisely controlled by different $V_G$. The inserts are the I-V curves of corresponding RESET operation. Ultra low switching current of nA level has been realized. (b) Retention characteristics of multi resistance states. (c) Repetitive switching cycles between different resistance states.

**S3. Temperature dependence of the cell resistance for** $V_G$<1.1V.

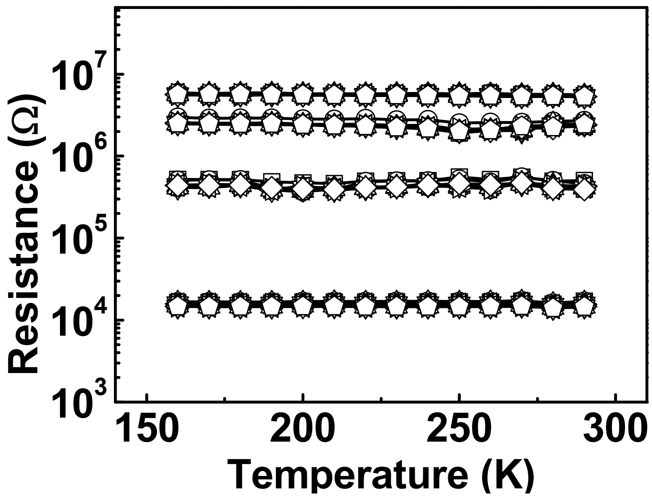


**Figure S3.** The cell resistance programmed achieved by $V_G<1.1V$. The independence of resistance on temperature was observed, indicating tunneling was the dominant conduction in these resistance states.

**S4. Estimation of the serial resistance on the quantized conduction.**

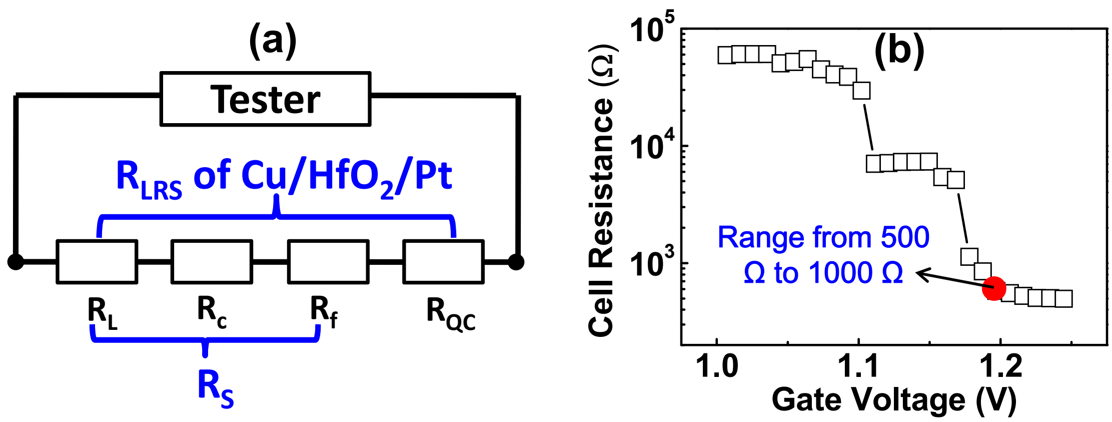


**Figure S4.** (a) Schematic of components of serial resistance ($R_S$). $R_L$ represents the line resistance in testing environment. $R_f$ is the resistance of filament from Cu side to its tip. $R_c$ is the contact resistance between filament and Cu electrode. (b) The cell resistance for $1V<V_G<1.25V$. The red dot represents the formation of complete filament. The resistance at this point can be approximately considered as a sum of $R_L$, $R_c$ and $R_f$. The typical value of $R_S$ ranges from 500 Ω to 1000 Ω.

**S5. EDS spectrums of CF region and non-CF region.**

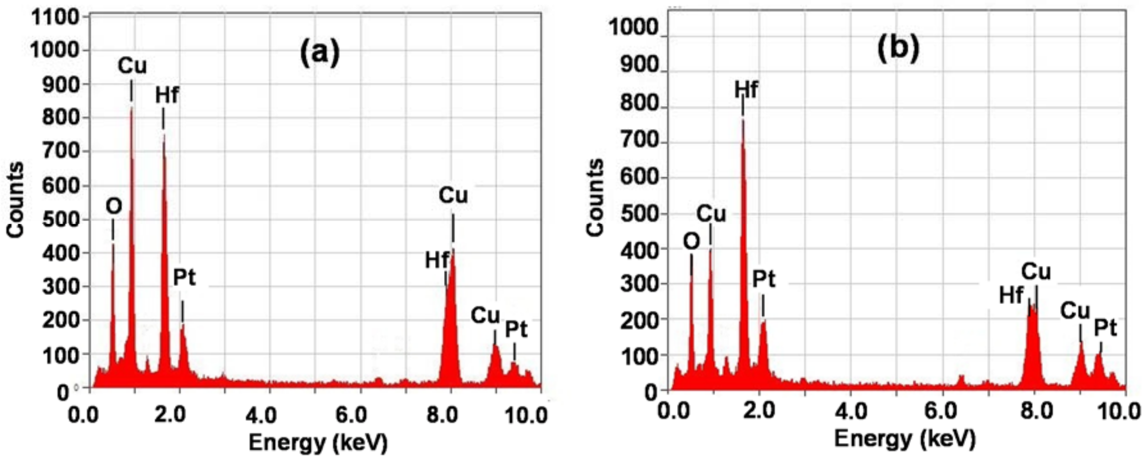


**Figure S5.** (a) CF region. (b) Non-CF region. The feature peaks of Cu signal in CF region is much higher than that in non-CF regions.

**S6.The voltage drop on cell during programming.**

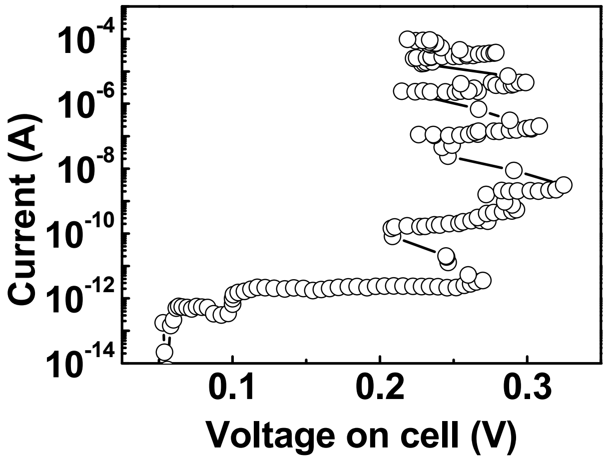


**Figure S6.** The $V_C$ can be directly detected by outputting the voltage of the bottom electrode.

**S7. Estimation of barrier height for electron transmission.**

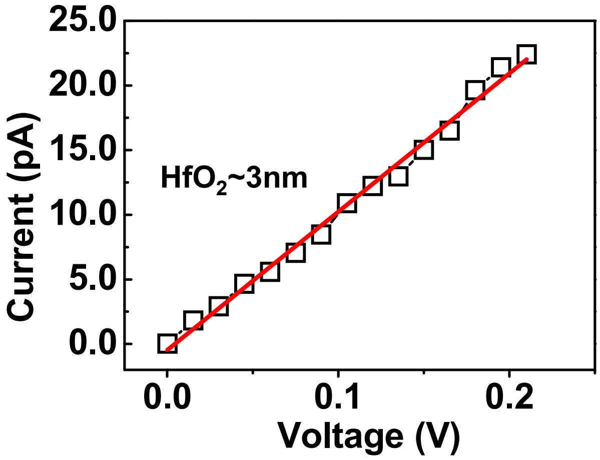


**Figure S7.** The I-V curve of fresh device with 3 nm $HfO_2$. The tunneling current from the filament tip to counter electrode can be expressed by: $I = A\frac{\sqrt{\bar{\phi}}}{\delta}\exp(-\frac{4\pi\delta}{h}\sqrt{2m_{eff}\bar{\phi}})V$ , where A is the area of tip, $\bar{\phi}$ is the barrier height, $\delta$ is the barrier width (gap length), $m_{eff}$ is the effective mass of electron and $h$ is the Planck constant. For the fresh cell, A is around 300 nm × 400 nm, $\delta$ =3 nm, and $m_{eff}$ =0.18$m_0$. (ref. IEEE TED 2011, 58, 2878.) The barrier height $\bar{\phi}$ (2.0 eV) can be obtained by fitting the I-V curve.

**S8. The simulation result of tunnel resistance versus gap length.**

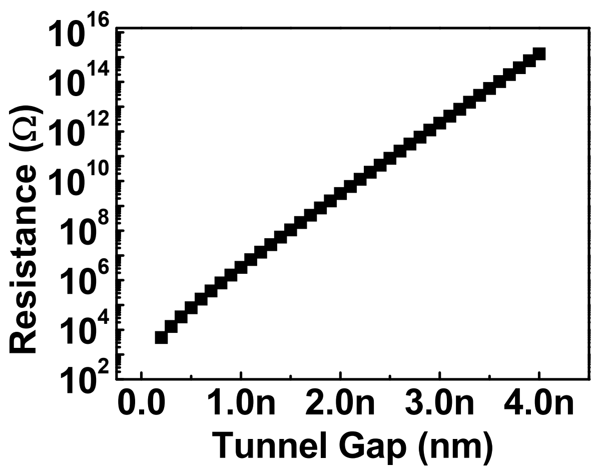


**Figure S8.** The resistance of tunnel gap, which can be calculated on the base of direct tunneling equation, with CF tip of 2.5 nm, $\bar{\phi}$=2.0 eV and $m_{eff}$ =0.18m$_0$.

**S9. Calculation of the filament length with different tip sizes.**

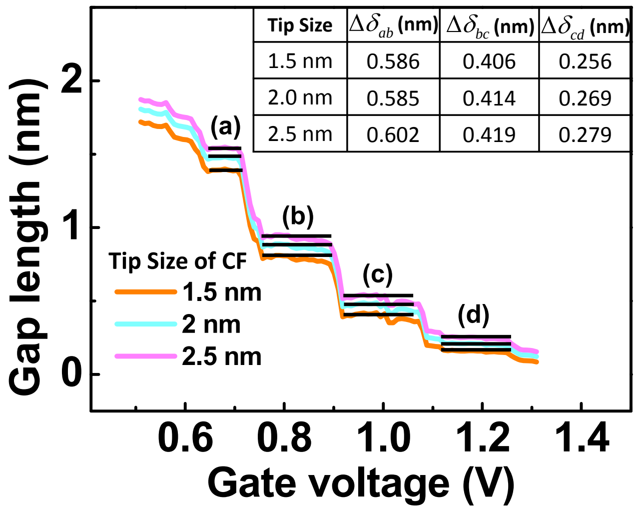


| Tip Size | $\Delta\delta_{ab}$ (nm) | $\Delta\delta_{bc}$ (nm) | $\Delta\delta_{cd}$ (nm) |
|---|---|---|---|
| 1.5 nm | 0.586 | 0.406 | 0.256 |
| 2.0 nm | 0.585 | 0.414 | 0.269 |
| 2.5 nm | 0.602 | 0.419 | 0.279 |

**Figure S9.** The relation of filament length with the gate voltage on the case of filament with different tip sizes. The increment of filament length was nearly independent of the tip size.